The Thermal Conductivity of 8 Yttria Stabilized Zirconia and Mullite Thermal Barrier Coating on Medium Carbon Steel Substrate

MSF Zaini, MS Adenan, JB Saedon, AMI Mamat

Abstract*: Thermal conductivity is one of the main features of a thermal barrier coating (TBC) that is important in making sure that the TBC gives its best functionality to the system. A good TBC has low thermal conductivity, so that the temperature can drop across the coating which allows the system to operate in extremely high temperatures. There are several factors that can influence the thermal conductivity of the TBC such as the type of ceramic material used, the deposition method and the physical features of the TBC itself. For this research, air plasma spray (APS) is used to deposit 8 wt% yttria stabilized zirconia (8YSZ) and mullite on medium carbon steel substrates to study their respective thermal conductivities. The aim here is to develop a heat shield using TBC to protect the electric motor in an electrical turbocompounding system. The characteristics of the deposited TBC such as microstructure, element composition, phases and thermal conductivity are studied. The thermal conductivity is reduced when medium carbon steel substrate deposited with TBC. The thermal conductivity of 8YSZ, mullite and uncoated sample at minute 60 is 0.868 W/mK, 0.903 W/mK and 1.057 W/mK, respectively. Therefore, the deposition of 8YSZ TBC can lower the thermal conductivity of the medium carbon steel heat shield.

***Keywords*: Thermal Conductivity, Mullite, 8 Yttria Stabilized Zirconia (8YSZ), Air Plasma Spray (APS)**

I. INTRODUCTION

A thermal barrier coating (TBC) is one of the ceramic coatings that is used on components or parts of a system to give an optimum protection to the system from the highest and most extreme operation temperature conditions. When TBC is deposited on certain components or parts, the heat that penetrates through it can be reduced as well as protect the system from damage and can also lengthen the lifetime of the components [1]. TBCs have been extensively used in high temperature applications such as in modern gas turbines and aircrafts in order to improve engine efficiency by enabling further increase of temperature during operation. This is because TBCs possess excellent thermal resistance [2]–[5]. A TBC can also be used as a resistances towards corrosion and oxidation of its metal substrate [6], [7]. Besides so, a TBC has its own attraction in the extreme temperature applications due to great wear resistance during its service [8].

A TBC is a multilayer coating that consists of ceramic top coat, metallic bond coat dan Thermally Grown Oxide (TGO) layer that forms during the operation of a TBC [9], [10]. At high temperature ambiences, TGO is formed between the bond coat and the top coat due to high contents of aluminum in the bond coat alloy which reacts with oxygen [11], [12]. Some of the researchers stated that the substrate itself is one of the layers in the TBC system [13], [14]. Each of the TBC layers have their very own function in the TBC to provide great service to the system and each TBCs are different from one another. Usually, the materials used for the metallic bond coat are MCrAlY where M is Ni, Co or both [2]. While the ceramic top coat is made up of yttria stabilized zirconia (YSZ).

There are several types of materials that can be used as top coat layers, but 8YSZ and mullite is the focus of this paper. The YSZ with wt% of 7-8 is the typical material used as top coats in TBCs which has contributed to the great performance of TBCs [15]–[17]. Some papers have stated that 6-8 wt% YSZ can be used as top coat [18]. There are several advantages of the YSZ material which are its high thermal expansion coefficient with metallic substrate, low thermal conductivity, low density, stable phase through high temperatures, good erosion resistance, excellent chemical inertness and good thermal shock resistance [2], [12], [15]. Depending on the temperature and size of its grains, a dense YSZ should attain thermal conductivity with a range of 0.6-3 W/mK and it will decrease when the temperature increases [2]. However, the disadvantages of a YSZ as a top coat material is that the sintering of YSZ is at extremely high temperatures which is above 1473 K, it reacts to oxygen, its phase transformation is at 1443 K and has susceptibility to corrosions [15], [17].

On the other hand, the aluminum silicate or mullite coatings show excessive thermal balance, excessive creep resistance in oxidative and corrosive environments, high resistance to crack propagation, high thermal shock resistance, and low thermal expansion [19]. Besides that, mullite coating is also not transparent to oxygen [15]. The mullite has higher thermal conductivity and more oxygen resistant compared to YSZ, which is why mullite is the best alternative for YSZ [15]. The lifespan of a mullite is longer than of a YSZ but above 1273 K, the lifetime of a mullite is generally shorter than that of a YSZ [15]. Other than that, the disadvantages of mullites is that it crystallizes at temperatures of 1023-1273 K that can cause cracking and the

Revised Manuscript Received on 20 October, 2019.
***** Correspondence Author
Muhammad Syazani Farhan bin Zaini, Faculty of Mechanical Engineering, Universiti Teknologi MARA, Shah Alam, Selangor, Malaysia
Mohd Shahriman bin Adenan*, Faculty of Mechanical Engineering, Universiti Teknologi MARA, Shah Alam, Selangor, Malaysia. Email: mshahriman@uitm.edu.my
Juri bin Saedon, Faculty of Mechanical Engineering, Universiti Teknologi MARA, Shah Alam, Selangor, Malaysia
Aman Mohd Ihsan bin Mamat, Faculty of Mechanical Engineering, Universiti Teknologi MARA, Shah Alam, Selangor, Malaysia

bonding of the coating will decrease [15]. The composition of a mullite is $3Al_2O_3.2SiO_2$ with the compounding of SiO_2 and Al_2O_3 [15]. Mullite coatings are suitable as an environmental barrier coating the top coat to protect the ceramic matrix composite because mullite coatings are stable in harsh chemical environments and its thermal expansion coefficient closer to their metal substrate [15], [19]. Mullite also has a good density and chemical compatibility [19].

The selection of TBC materials is important and are restricted to several properties and characteristic such as low thermal conductivity, high melting point, high wear resistant, hardness, a good adherence with substrate, and chemical inertness [17], [20]. A low thermal conductivity is a substantial characteristics that each TBC material must have to ensure that the heat flow rate can be reduced or resisted from entering the substrate. The TBC materials must have a high melting point so that the system can operate in extreme temperatures. Besides that, in terms of high wear resistance, TBC materials must have resistance towards oxidation and corrosion. A TBC is used to protect the components and parts for heavy applications whereby the materials used as TBC layers must possess the best range of a micro and macro hardness. Also, the adhesion of TBC layers must be good and strong with its substrate to make sure that the bonding is excellent. Other than that, the materials to be used as TBC layers must be inert to chemicals avoid reaction with the any chemicals during its operation.

A TBC with low thermal conductivity is the main goal in getting a great TBC with excellent performance. This paper reports the TBC is developed on a medium carbon steel substrate by using an Air Plasma Spray (APS) method where it applies as heat shields to protect electric motor in an electrical turbocompounding system. There are two types of top coat materials used in this research which are 8YSZ and mullite to determine which TBC has the lowest thermal conductivity. The morphology, phases of the coating after spray and the thermal conductivity of both samples are explained in this paper.

II. METHODOLOGY

The substrate used in this research for morphology, phases and thermal conductivity study is medium carbon steel (AISI 1050) with dimensions of 200 mm x 100 mm x 2 mm. The substrate surface is cleaned first before the deposition process is performed. A thinner solution is used to clean the substrate from undesirable residues such as impurities and lubricants. After that, the substrate is blasted using Al2O3 with a mix of mesh 16 and 24. The cleaned medium carbon steel substrate is deposited with NiCoCrAlY (wt % of Ni-23Co-17Cr-12Al-0.5Y) bond coat via an APS method; obtaining a thickness of 100 µm. Then, 8YSZ and mullite top coat with 250 µm of thickness is deposited onto the bond coat using the APS method as well. The parameters used for the deposit of the top coats and bond coat via APS are stated in Table-I.

The as-sprayed TBC sample is cut into a cross-section with a size of 15 mm x 5 mm. The microstructures of cross-sectional as-sprayed TBC are observed using a Scanning Electron Microscope (SEM, Hitachi SU3500) equipment. Simultaneously, EDX analyses are executed to obtain the element composition in the TBC layers using an x-ray detector attached with the SEM equipment. The x-ray diffractometer (Rigaku Ultima IV) with Cu Kα radiation is used to perform XRD analyses in order to examine the phases of the as-sprayed TBCs. The thermal conductivity of the TBC samples is obtained using Fourier's Law of Heat Conduction (1). Where, Qcond, is the amount of heat transfer, k, is the thermal conductivity, A, is the cross-sectional area, dT, is the temperature difference and dt, is the thickness of the sample. The dT values are obtained from a heat conduction test performed with the heat conduction apparatus. Fig. 1 is the heat conduction apparatus.

$$Q_{cond} = -kA\frac{dT}{dt} \quad (1)$$

The as-sprayed TBC with mullite and 8YSZ top coat is cut into smaller sizes and then clamped between the hot part and cold part of the heat conduction apparatus. The temperature readings are collected at 6 points which are point 1, 2 and 3 in the hot part, and point 4, 5 and 6 in cold part. These readings are taken to determine the temperature difference across the clamped sample. The readings are taken at every 5 minutes for 1 hour and it starts when the temperature reaches 55°C. The test is repeated 3 times and the thermal conductivity is obtained from the formula. The results for the thermal conductivity of the coated samples are compared to the uncoated sample that is tested in the same apparatus to verify the effect of TBC in decreasing thermal conductivity.

Fig. 1.Heat conduction apparatus

Table-I: The parameters used for spraying bond coat and top coat.

Items	Bond coat	Top coat
Current (A)	600	600
Electric power (kW)	40	30
Stand-off distance (mm)	140	90
Powder feed rate (g/min)	30	25

III. RESULT AND DISCUSSION

The microstructure of TBC with different top coat material can be seen in the SEM image shown in Fig. 2. From the SEM image, it clearly shows that the TBCs are uniformly deposited on their medium carbon steel substrates without any cracks and is attached orderly. Also, the SEM image proves that the APS produced ceramic coatings with lamellar microstructure compared to the Electron Beam-Physical Vapor Deposition (EB-PVD) which produced columnar microstructure [21],

[22]. From the observation, there are a lot of micro-pores in the 8YSZ and mullite ceramic coatings as shown in the SEM images. This is because the APS produces ceramic coatings with unorganized micro-pores [9]. From the SEM image, the microstructure of mullite coating has large pores compared to 8YSZ coatings. This shows that there is a weak bond between the mullite particles. In APS ceramic coating, due to the polishing effect from sample polishing for microstructure analysis, it removes the weak bonded particles and cause large pores [23].

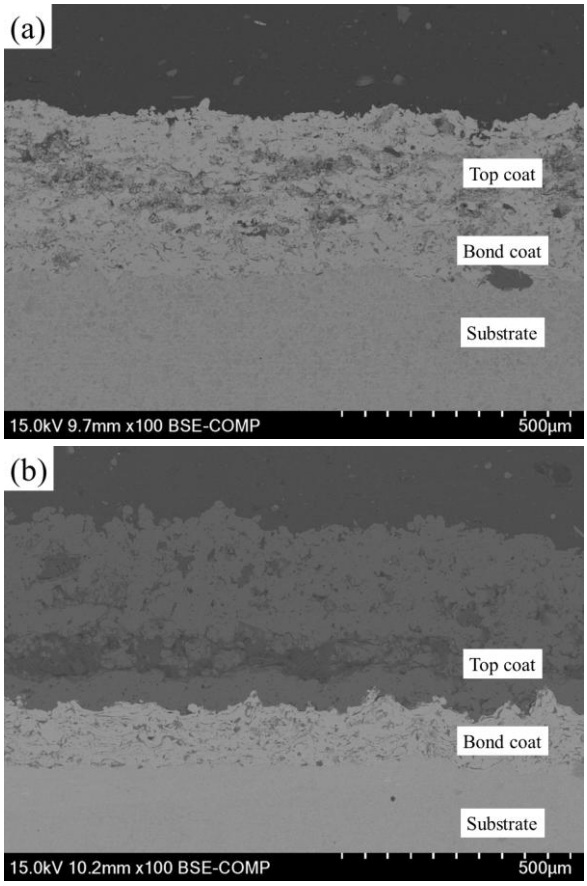

Fig. 2.The SEM image of (a) 8YSZ and (b) mullite sample

The EDX analysis is done on the as-sprayed TBC samples to determine the element contents of the coating. The EDX analysis is done via the SEM image after the samples are examined for microstructure analyses. Fig. 3(a) is the SEM image of 8YSZ sample with EDX spot markings for element composition analysis. Here, spot 1, spot 2, spot 3 and spot 4 are located at the top coat layer, top coat-bond coat interface, bond coat layer and the interface of bond coat-substrate. The results of the EDX analysis for 8YSZ sample is shown on Fig. 4. The elements contained in spot 1 are 8YSZ top coat element which is Zr, Y and O with wt% 63.4 wt%, 7.5 wt% and 29.1 wt%, respectively. The Y element decreases after the deposition process because the Y element in only 8 wt% present in the 8YSZ powder. The elements contained in spot 2 is Zr, Y, O, Ni, Co, Cr and Al. The bond coat elements do not appear much on the interface between top coat and bond coat. The Zr and Y elements decreased to 53.6 wt% and 6.2 wt%, respectively, in spot 2. The content of O element remains constant even after the deposition process. In addition, the element contents for the bond coat on spot 3 are unexpected because the wt% of Al is very high which is 42.8 wt% higher than 12 wt% in the bond coat powder. Still in spot 3, there is a presence of the O element with 35.9 wt%. The presence of the O element can cause the oxidation to the TBC and subsequently lead to failure. Moving on, spot 4 shows the presence of the bond coat and substrate elements such as Ni, Co, Cr, Al, Y, Mn, Fe, Si, and C. Out of all these elements, the highest presence of element is the Ni element with 35.3 wt%.

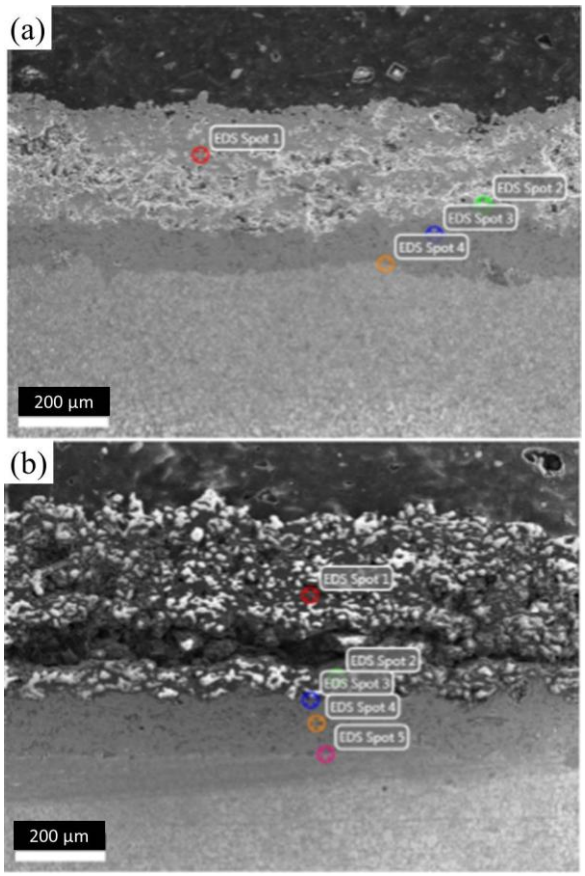

Fig. 3.The EDX spot for (a) 8YSZ and (b) mullite sample

Different from the 8YSZ sample, the results of the EDX analysis for the mullite sample is shown on Fig. 5. The locations of EDX spots for the mullite sample were shown in Fig. 3(b). There, spot 1 which is located at the mullite top coat shows the elements Al, Si and O appearance with the wt% of 40.4 wt%, 9.7 wt% and 50.0 wt%, respectively. In addition, the wt% of elements Al and Si increases to 41.7 wt% and 10.5 wt%, respectively, at spot 2 which is approaching the interface of top coat and bond coat. On the other hand, the wt% of element O at spot 2 decreases across the TBC after the deposition process. The elements that appear at spot 1 and 2 are the same because of the location of spot 1 and 2 that is at the top coat layer. The element that appeared at spot 3 are of the top coat and bond coat elements which are Ni, Cr, Co, Al and Y including O, Si and C element with the wt% of 0.7 wt%, 1.0 wt%, 1.2 wt%, 26.8 wt%, 0.1 wt%, 38.0 wt%, 5.9 wt% and 26.4 wt%, respectively. These elements appeared because of the interface of top coat and bond coat. The element with the highest content in spot 3 is O and the element with the lowest content is Y. The wt% for element Ni, Cr, Co and Y increases at spot 4 with 48.6

wt%, 17.8 wt%, 22.5 wt% and 0.3 wt%, respectively. While, the wt% for element Al decreases from 26.8 wt% at spot 3 to 9.6 wt% at spot 4. At spot 5, which is the interface of the bond coat and substrate has a higher content of Ni element compared to the bond coat itself.

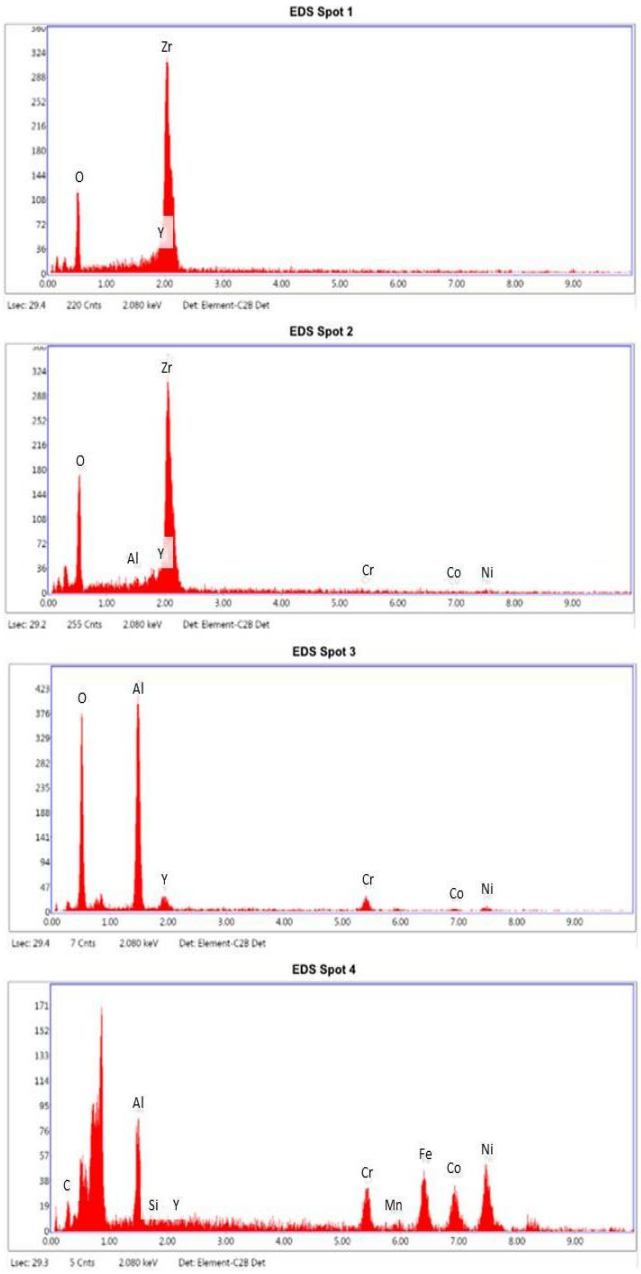

Fig. 4.The EDX analysis at different spot for 8YSZ sample

The phase composition of the TBCs after deposition on the substrates are analysed using the X-ray diffractometer. The 8YSZ and mullite samples are cut into small sizes before the XRD analysis. From Fig. 6, it is shown that the XRD pattern of the 8YSZ sample matched with the phases of standard PDF diffraction card for zirconium yttrium oxide (PDF # 01-070-4429). This shows that the XRD pattern of 8YSZ did not change much during the deposition of 8YSZ on the bond coated medium carbon steel substrate. The XRD pattern of 8YSZ sample is similar to other researchers' results [24]. The zirconium yttrium oxide (ZrY_2O_5) phases formed at the peak of (1,0,1), (0,0,2), (1,1,0), (1,1,2), (2,0,0), (1,0,3), (2,1,1), (2,0,2) and (2,2,0).

For the mullite sample, the XRD patterns of its phases are shown in Fig. 7. The XRD pattern for the mullite sample after the deposition process is similar with the results from other researchers [23]. The XRD peak of the mullite sample matched with the standard PDF diffraction card for mullite (PDF # 01-079-1456). The XRD patterns of mullite also did not change much during the deposition of mullite on the medium carbon steel substrate. The phase of peak (1,2,0), (2,2,0), (2,3,0), (0,4,1) and (3,3,1) is a mullite ($3Al_2O_3.2SiO_2$) phase.

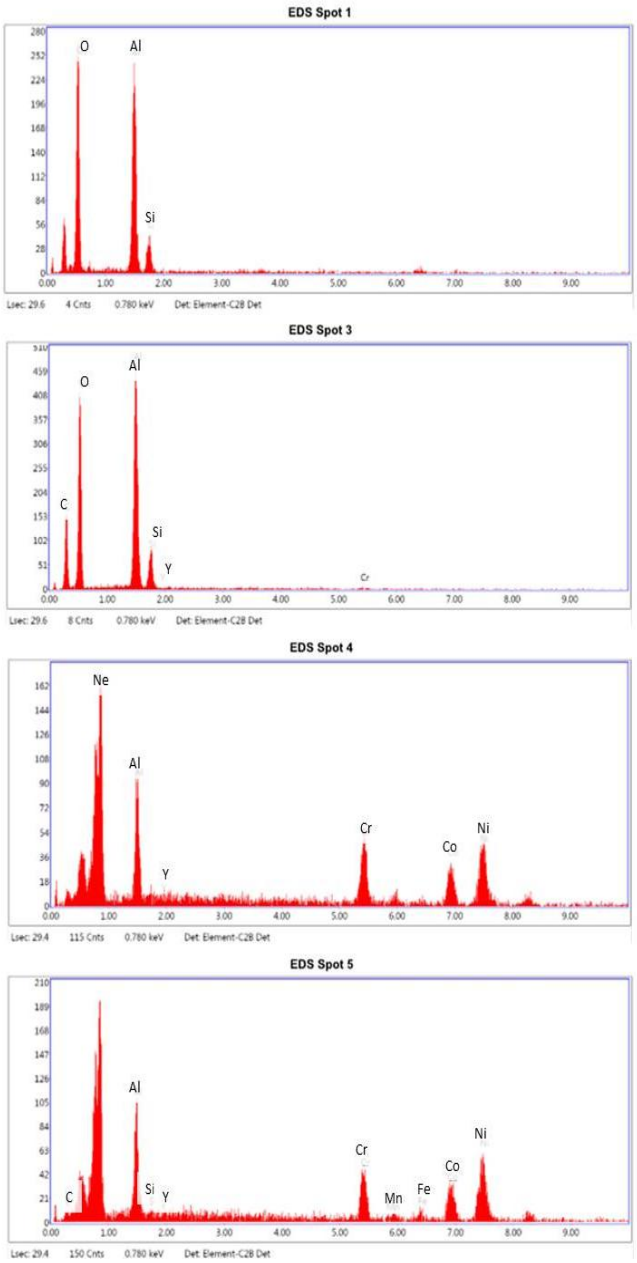

Fig. 5.The EDX analysis at different spot for mullite sample

The results for the thermal conductivity of the as-sprayed TBCs with 8YSZ and mullite top coats, respectively, is shown in Fig. 8. From the thermal conductivity results, it clearly shows that the thermal conductivity decreases after TBCs are applied to the medium carbon steel substrates.

The thermal conductivity of 8YSZ sample at minute 60 is 0.868 W/mK which is lower than the thermal conductivity of mullite sample 0.903 W/mK at minute 60. While the thermal conductivity of the uncoated sample at minute 60 is quite high compared to 8YSZ and mullite sample which is 1.057 W/mK. The thermal conductivity of uncoated sample is higher than of the TBC samples because there are no ceramic coatings on it to shield the heat from penetrating the sample during testing. Other than that, the thermal conductivity of TBC coated samples are low due to the interface disorder that scatter phonons at the grain boundaries caused by pores and the small grains in the ceramic coating [13]. The thermal conductivity is reduced by 0.189 W/mK when the TBC with 8YSZ top coat is applied to the medium carbon steel substrate. On the other hand, only 0.154 W/mK of the thermal conductivity is reduced when the TBC with the mullite top coat is applied. One of the characteristic of mullite is that it has a higher thermal conductivity rate compared to YSZ [15].

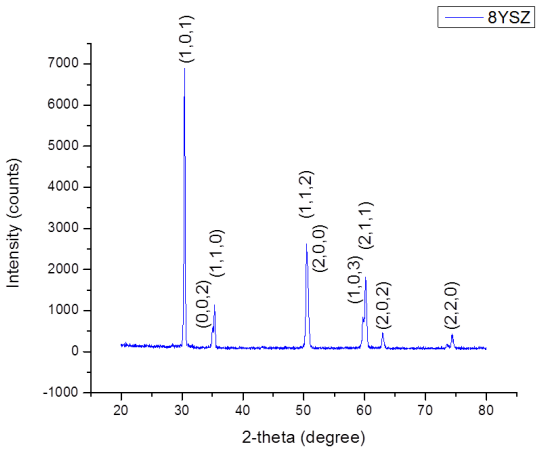

Fig. 6.The XRD pattern for 8YSZ sample

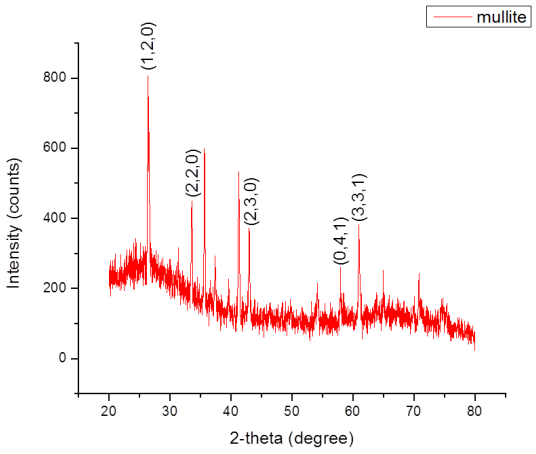

Fig. 7.The XRD pattern for mullite sample

From the thermal conductivity results of coated and uncoated sample, it clearly shows that the deposition method also influenced the thermal conductivity of the ceramic coated substrate. This is because a common APS method produced a coating with a microstructure characteristics that consist of cracks and pores with the level of porosity of 10–30%, that can decrease a coatings thermal conductivity to less than 1 W/mK [25]. The presence of porosity very useful to reduce thermal conductivity values. Besides that, the competent thermal conductivity for TBCs varies widely, where usually for APS coatings it is 0.9 to 1.4 W/mK and for EB-PVD coatings it is 1.8 to 2.0 W/mK [2]. Even though the method of measuring the thermal conductivity of the TBC samples is not really accurate, the results still show that the thermal conductivity of the samples decreased when it is deposited with TBC. The most acceptable method to measure thermal conductivity of TBC is laser flash analysis LFA [26].

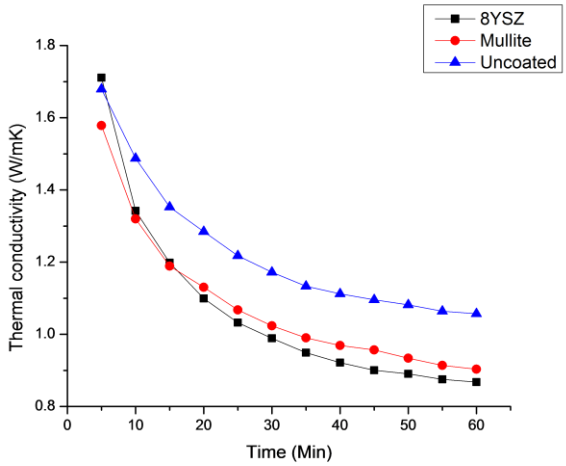

Fig. 8. The thermal conductivity of coated and uncoated sample

IV. CONCLUSION

The TBCs with 8YSZ and mullite top coats are successfully deposited on medium carbon steel substrates. The microstructure, element composition, phases and thermal conductivity of the TBCs were examined. Therefore, some of the conclusions that can be highlighted are:

- The 8YSZ and mullite coatings are uniformly deposited on medium carbon steel substrate.
- The element that appeared on the 8YSZ and mullite top coat after being deposited on the substrates are the element composition of the powder itself.
- The XRD patterns of 8YSZ and mullite sample are the same with the XRD patterns from others researchers and its peaks matched the phases of standard PDF diffraction card for zirconium yttrium oxide (PDF # 01-070-4429) and mullite (PDF # 01-079-1452). The ZrY_2O_5 and $3Al_2O_3.2SiO_2$ formed at the peak of XRD patterns.
- Both the depositions of 8YSZ and mullite on their respected TBCs can lower the thermal conductivity of the medium carbon steel sample. However, the 8YSZ coating has the lower thermal conductivity value compared to one of the mullite coating

ACKNOWLEDGMENT

The authors would like to thank Ministry of Education Malaysia (MOE) for providing the Prototype Development Reseach Grant Scheme (PRGS) as support fund to complete this research. This is also to acknowledge the Faculty of Mechanical Engineering, Universiti Teknologi MARA (UiTM) for providing technical support to conduct this research.

REFERENCES

1. Z. Xu, Z. Wang, G. Huang, R. Mu, and L. He, "Morphology, bond strength and thermal cycling behavior of (Ni, Pt)Al/YSZ EB-PVD thermal barrier coatings," *J. Alloys Compd.*, vol. 651, pp. 445–453, 2015.
2. Y. Wang, J. Li, H. Liu, and Y. Weng, "Study on thermal resistance performance of 8YSZ thermal barrier coatings," *Int. J. Therm. Sci.*, vol. 122, pp. 12–25, 2017.
3. L. Yang, H. L. Li, Y. C. Zhou, W. Zhu, Y. G. Wei, and J. P. Zhang, "Erosion failure mechanism of EB-PVD thermal barrier coatings with real morphology," *Wear*, vol. 392–393, no. January, pp. 99–108, 2017.
4. C. Cai, S. Chang, Y. Zhou, L. Yang, G. Zhou, and Y. Wang, "Microstructure characteristics of EB-PVD YSZ thermal barrier coatings corroded by molten volcanic ash," *Surf. Coatings Technol.*, vol. 286, pp. 49–56, 2016.
5. G. Mauer, D. Sebold, R. Vaßen, E. Hejrani, D. Naumenko, and W. J. Quadakkers, "Impact of processing conditions and feedstock characteristics on thermally sprayed MCrAlY bondcoat properties," *Surf. Coatings Technol.*, vol. 318, pp. 114–121, 2017.
6. M. H. Li, X. F. Sun, S. K. Gong, Z. Y. Zhang, H. R. Guan, and Z. Q. Hu, "Phase transformation and bond coat oxidation behavior of EB-PVD thermal barrier coating," *Surf. Coat. Technol.*, vol. 176, pp. 209–214, 2004.
7. H. Guo, Y. Cui, H. Peng, and S. Gong, "Improved cyclic oxidation resistance of electron beam physical vapor deposited nano-oxide dispersed b-NiAl coatings for Hf-containing superalloy," *Corros. Sci.*, vol. 52, no. 4, pp. 1440–1446, 2010.
8. J. Wan *et al.*, "Fracture characteristics of freestanding 8wt% Y2O3-ZrO2coatings by single edge notched beam and Vickers indentation tests," *Mater. Sci. Eng. A*, vol. 581, pp. 140–144, 2013.
9. H. R. Abedi, M. Salehi, and A. Shafyei, "Microstructural, mechanical and thermal shock properties of triple-layer TBCs with different thicknesses of bond coat and ceramic top coat deposited onto polyimide matrix composite," *Ceram. Int.*, vol. 44, no. 6, pp. 6212–6222, 2018.
10. K. Torkashvand, E. Poursaeidi, and M. Mohammadi, "Effect of TGO thickness on the thermal barrier coatings life under thermal shock and thermal cycle loading," *Ceram. Int.*, no. December 2017, 2018.
11. [11] C. Nordhorn, R. Mücke, D. E. Mack, and R. Vaßen, "Probabilistic lifetime model for atmospherically plasma sprayed thermal barrier coating systems," *Mech. Mater.*, vol. 93, pp. 199–208, 2016.
12. J. Wang *et al.*, "Effect of spraying power on microstructure and property of nanostructured YSZ thermal barrier coatings," *J. Alloys Compd.*, vol. 730, pp. 471–482, 2018.
13. [13] K. Jiang, S. Liu, and X. Wang, "Phase stability and thermal conductivity of nanostructured tetragonal yttria–stabilized zirconia thermal barrier coatings deposited by air–plasma spraying," *Ceram. Int.*, vol. 43, no. 15, pp. 12633–12640, 2017.
14. R. Darolia, "Thermal barrier coatings technology: critical review, progress update, remaining challenges and prospects," *Int. Mater. Rev.*, vol. 58, no. 6, pp. 315–348, 2013.
15. X. Q. Cao, R. Vassen, and D. Stoever, "Ceramic materials for thermal barrier coatings," *J. Eur. Ceram. Soc.*, vol. 24, no. 1, pp. 1–10, 2004.
16. H. Peng, L. Wang, L. Guo, W. Miao, H. Guo, and S. Gong, "Degradation of EB-PVD thermal barrier coatings caused by CMAS deposits," *Prog. Nat. Sci. Mater. Int.*, vol. 22, no. 5, pp. 461–467, 2012.
17. S. Barnwal and B. C. Bissa, "Thermal Barrier Coating System and Different Processes to apply them-A Review," *Int. J. Innov. Res. Sci. Eng. Technol. (An ISO Certif. Organ.*, vol. 3297, no. 9, pp. 8506–8512, 2007.
18. X. W. Chen, C. Y. Zhao, and B. X. Wang, "Microstructural effect on radiative scattering coefficient and asymmetry factor of anisotropic thermal barrier coatings," *J. Quant. Spectrosc. Radiat. Transf.*, vol. 210, pp. 116–126, 2018.
19. V. Kumar and B. Kandasubramanian, "Processing and design methodologies for advanced and novel thermal barrier coatings for engineering applications," *Cardiovasc. Res.*, pp. 1–28, 2016.
20. A. M. Noor, M. R. Abbas, M. B. Uday, and S. Rajoo, "Improving thermal efficiency of an automotive turbocharger turbine with ceramic," in *International Conference on Innovative Technologies, IN-TECH 2016*.
21. Z. X. Yu, J. B. Huang, W. Z. Wang, J. Y. Yu, and L. M. Wu, "Deposition and properties of a multilayered thermal barrier coating," *Surf. Coatings Technol.*, vol. 288, pp. 126–134, 2016.
22. M. S. Sahith, G. Giridhara, and R. S. Kumar, "Development and analysis of thermal barrier coatings on gas turbine blades - A Review," *Mater. Today Proc.*, vol. 5, no. 1, pp. 2746–2751, 2018.
23. S. Li, X. Zhao, Y. An, W. Deng, G. Hou, E. Hao, H. Zhou, and J. Chen, "Effect of deposition temperature on the mechanical, corrosive and tribological properties of mullite coatings," *Ceram. Int.*, vol. 44, no. 6, pp. 6719–6729, 2018.
24. R. Ghasemi and H. Vakilifard, "Plasma-sprayed nanostructured YSZ thermal barrier coatings: Thermal insulation capability and adhesion strength," *Ceram. Int.*, vol. 43, no. 12, pp. 8556–8563, 2017.
25. S. Tailor, R. Upadhyaya, S. Y. Manjunath, A. V. Dub, A. Modi, and S. C. Modi, "Atmospheric plasma sprayed 7%-YSZ thick thermal barrier coatings with controlled segmentation crack densities and its thermal cycling behavior," *Ceram. Int.*, vol. 44, no. 3, pp. 2691–2699, 2018.
26. K. Torkashvand, E. Poursaeidi, and J. Ghazanfarian, "Experimental and numerical study of thermal conductivity of plasma-sprayed thermal barrier coatings with random distributions of pores," *Appl. Therm. Eng.*, vol. 137, pp. 494–503, 2018.

AUTHORS PROFILE

Muhammad Syazani Farhan bin Zaini is currently doing his Master of Science (Mechanical Engineering) in Universiti Teknologi MARA. He received his degree from Universiti Kebangsaan Malaysia with Bachelor of Engineering (Manufacturing Engineering) in 2017. His research is focusing on Thermal Barrier Coating (TBC) on medium carbon steel heat shield for electrical turbocompounding system. In his research, he uses two types of top coat materials that are deposited on medium carbon steel substrates to determine the most suitable material for TBC in heat shielding applications.

Mohd Shahriman bin Adenan (Dr.) is currently working as a Senior Lecturer with the Faculty of Mechanical Engineering, Universiti Teknologi MARA Shah Alam, where he has been working since 2008. He received his Bachelor of Engineering and Master of Engineering from Universiti Malaya; and received his Ph.D in Mechanical Engineering from UiTM in 2015. His research interests are concerning surface engineering and virtual manufacturing. Much of his work focuses on improving surface properties of stainless steel for oil and gas industry and biomedical applications. Currently, he is exploring new ventures in virtual manufacturing technology, focusing on material modelling for automotive parts production.

Juri bin Saedon (Dr.) is currently working as a Senior Lecturer with the Faculty of Mechanical Engineering, Universiti Teknologi MARA Shah Alam, where he has been working since 1996. Before that, he was a teacher at Sekolah Teknik Kuala Lumpur from 1990 until August 1996. He received his Bachelor of Technology and Education in Mechanical Engineering from Universiti Teknologi Malaysia. Then he completed his Master of Science and Ph.D in Mechanical and Manufacturing respectively from the University of Birmingham, United Kingdom. His expertise is in the field of manufacturing processes focusing on the CAD/CAM, CAE, and product design. Furthermore, his research interests are in the field of micromachining, machinability-conventional and non-conventional machining.

Aman Mohd Ihsan bin Mamat (Assoc. Prof. Dr.) is currently working as a Senior Lecturer with the Faculty of Mechanical Engineering, Universiti Teknologi MARA Shah Alam, where he has been working since 2004. He was also appointed as the Head of Graduate Studies (Research Programme) at the Institute of Graduate Studies, Uiversiti Teknologi MARA. He received his Bachelor of Engineering in Mechanical Engineering (Aeronautics) from Universiti Teknologi Malaysia. He also completed his Mastere Specialize in Techniques Aeronautique et Spatials (Aeronautics) from Ecolé Nationale de l'Aeronaique et De l'Espace (ENSAE), Toulouse, France and Ph.D in Mechanical Engineering from Imperial College, London. His expertise is in thermofluids and energy. His research interests are in automotive and aerospace powertrain, energy recovery, turbomachinery and heat transfer.